N95-21752

345746

AN ASSESSMENT OF IMAGE RECONSTRUCTION FROM BALLOON-BORNE AND THE IRAS DATA

S.K. GHOSH, B. DAS, T.N. RENGARAJAN AND R.P. VERMA
Tata Institute of Fundamental Research, Homi Bhabha Road, Bombay 400005 INDIA

ABSTRACT Angular resolution and structural information from the far-infrared mapping of astronomical sources (Galactic star forming regions, spiral galaxies etc.) made using the TIFR 1 m balloon-borne telescope and the IRAS have been compared. The effective wavelengths of the TIFR two-band photometer are 58 and 150 μm. From IRAS, the survey COADD data, additional observations (AOs) made with the survey detectors with different Macros (DPS, DSD, DPM), as well as the chopped photometric channel (CPC) data have been considered here. The observed signals have been processed using different deconvolution strategies, either based on a maximum entropy method (MEM) developed at TIFR or the HiRes package developed at IPAC. Relative merits of each of these, under different conditions of signal to noise ratio, are highlighted. The following sources have been selected for illustration: Carina complex, W31 region, IRAS 10361–5830 (all Galactic), M101 and M81 (extragalactic). The main conclusions are: far-infrared maps from MEM deconvolution of balloon-borne data have the best angular resolution; MEM deconvolution of IRAS AOs gives resolution comparable to HiRes but with less amount of computation, though the dynamic range in MEM maps is less than in HiRes maps.

INTRODUCTION

At the far-infrared wavelengths, observations are made by telescopes aboard aircrafts, balloons, rockets and satellites. These telescopes are of moderate size ($\leq$ 1 m) and generally the field of view is several arcminutes (except in the case of Kuiper Airborne Observatory where the field of view is less than 1′). Therefore, there is a need for increasing the resolution by signal processing. Many techniques have been used to improve the resolution of the maps. In this paper we compare three of these techniques – two based on the maximum entropy method (MEM) and the third one, HiRes, based on maximum correlation method (MCM).

OBSERVATIONS AND DATA ANALYSIS

The data used are taken from balloon flights made with the Tata Institute of Fundamental Research (TIFR) 1 m telescope and from the IRAS satellite. The

S. Terebey and J. Mazzarella (eds.), *Science with High-Spatial Resolution Far Infrared Data*, 17–22, 1994, Jet Propulsion Laboratory, Pasadena, CA.

TIFR balloon-borne telescope is an f/8 cassegrain telescope with metal mirrors. The field of view is 2'.4 diameter and the radiation is chopped along the cross-elevation (XEL) axis by vibrating the secondary mirror at a frequency of 20 Hz and with an amplitude of 3'.6. A one band photometer with an effective wavelength of 150 μm and a two band photometer with effective wavelengths of 58 and 150 μm have been used. Mapping is done by raster scanning an area of $\sim$ 30' x 30' by scanning along the XEL axis at a typical rate of 0'.75 s^{-1} and steps of 1'.4 in elevation (EL). Far-infrared signals are passed through a digital filter to reduce the noise and then gridded in XEL-EL plane with pixel size of 0'.3 x 0'.3. Two dimensional deconvolution is performed on these signals using a MEM procedure based on Gull and Daniell (1978). The code for this MEM deconvolution has been developed at TIFR. The point spread profile (PSP) has been obtained using the observations of the planets. Hereafter, this procedure is referred to as MEM(a). The resolution in the deconvolved maps is $\sim$ 1'.2 and typical dynamic range for good signal to noise ratio is $\sim$ 100. The computing time for deconvolving a 1° x 1° field is $\sim$ 1 hour per band on a PC 486. Further details of the telescope and the data processing are given in Ghosh et al. (1988).

The sizes of the IRAS survey detectors along the cross-scan direction are $\geq$ 4'.5; along the in-scan direction the sizes are 0'.75 at 12 and 25 μm, 1'.5 at 60 μm and 3'.0 at 100 μm. There are a few edge detectors with smaller size along the cross-scan direction– 0'.75 at 12 and 25 μm, 1'.5 at 60 μm and 3'.0 at 100 μm (IRAS Catalogs and Atlases, Explanatory Supplement, 1988). In the CPC, the detectors have a circular field of view with a diameter of 1'.2 at 50 and 100 μm. Besides the survey data, there are additional observations (AOs) with smaller cross-scan steps and generally slower scan rate leading to higher signal to noise ratio (SNR). Data from the IRAS satellite are available in several forms. These are – Survey COADD grids, AO grids with different Macros, CPC data and calibrated reconstructed detector data (CRDD). For the first three of these sets, the signals from different detectors in the given band are mixed, therefore for the deconvolution one has to use an average PSP. In the CRDD, the signals from different detectors are kept separate, therefore the characteristics of individual detectors can be used.

We have deconvolved data from survey COADDs, AOs with different Macros and the CPC data, using a self adaptive scheme using MEM based on Skilling and Bryan (1984). The PSPs are derived from the observations of point sources (NGC 6543, asteroids). The resolution in the deconvolved map depends on the wavelength and the nature of the input grid. The FWHM size for the deconvolved map of a point source for some of the grids is given in Table 1. The dynamic range for a good SNR is $\sim$ 300. The computing time for deconvolving a 1° x 1° field is less than 30 minutes per band on a PC 486. The above procedure is referred to as MEM(b). Details of this procedure along with the deconvolved maps for 18 large galaxies based on data from the AOs and the CPC can be found in Ghosh et al. (1993).

The CRDD data are processed using the HiRes routine which is based on a maximum correlation method. Here the pixel size is much smaller, 15" $\times$ 15". The input image is "cleaned" and "flat fielded" before processing further to remove various artifacts. The digitized spatial response function, the detector sky position and the orientation for each detector are used to calculate the correction factors iteratively. The details of this technique are given by Aumann, Fowler

TABLE 1 FWHM size for a point source.

Grid	Processing	FWHM Size (in-scan x cross-scan) 12 μm	25 μm	50/60 μm	100 μm
AO DPS02B	MEM(b)	$\leq 0'.5 X 0'.7$	$\leq 0'.5 X 0'.7$	$0'.6 X 1'.0$	$1'.4 X 1'.7$
AO DSD01A	MEM(b)	$\leq 0'.5 X 0'.5$	$\leq 0'.5 X 0'.5$	$\leq 0'.5 X 0'.5$	$0'.9 X 1'.2$
CPC	MEM(b)	...	...	$\leq 0'.3 X 0'.4$	$\leq 0'.5 X 0'.4$
	HiRes [a]	$0'.4 X 0'.6$	$0'.4 X 0'.6$	$0'.7 X 1'.0$	$1'.3 X 1'.6$

[a]From Rice (1993)

and Melnyk (1990). The resolution in the processed maps after 20 iterations is given in Table 1. The processing time on a Sun Sparc2 (for 20 iterations) for a 1° x 1° field is more than 30 minutes for each band.

RESULTS

Some of the maps obtained using different procedures are presented here for illustration. First we consider Galactic HII/star-forming regions. In Figures 1, 2 and 3 we give the maps of a region in the Carina nebula, around IRAS 10361–5830 and W31 respectively generated from balloon-borne observations deconvolved with MEM(a) and compare these with the maps obtained from the IRAS data with HiRes processing (for Carina) and MEM(b). Most of the sources in the the two sets of maps are reproduced rather well. However the superior resolution of the maps from balloon-borne observations for these complex regions is quite clear.

Next we present some examples of the maps of large galaxies. In Figures 4 and 5 we give the maps for the galaxies M101 and M81 respectively, generated from AO data deconvolved with MEM(b) and compare these with the maps processed with HiRes routine. HiRes maps are taken from Rice (1993). One can see that the two sets of maps are remarkably similar. Specifically, in the case of M101 galaxy, the HII regions resolved in the HiRes maps are equally well resolved in the MEM(b) maps.

CONCLUSIONS

1. The angular resolution of maps obtained from TIFR balloon-borne measurements at 150 μm is better than or comparable to that from HiRes at 100 μm. This is mainly due to smaller field of view of the balloon-borne photometer. It may be mentioned that for our future balloon flights we will be using a new photometer with liquid ^3He cooled bolometer arrays. This two band photometer will have a field of view of 1'.6 and effective wavelengths of $\sim$ 130 and 200 μm. This will give further improvement in angular resolution besides going to longer wavelengths and higher sensitivity.

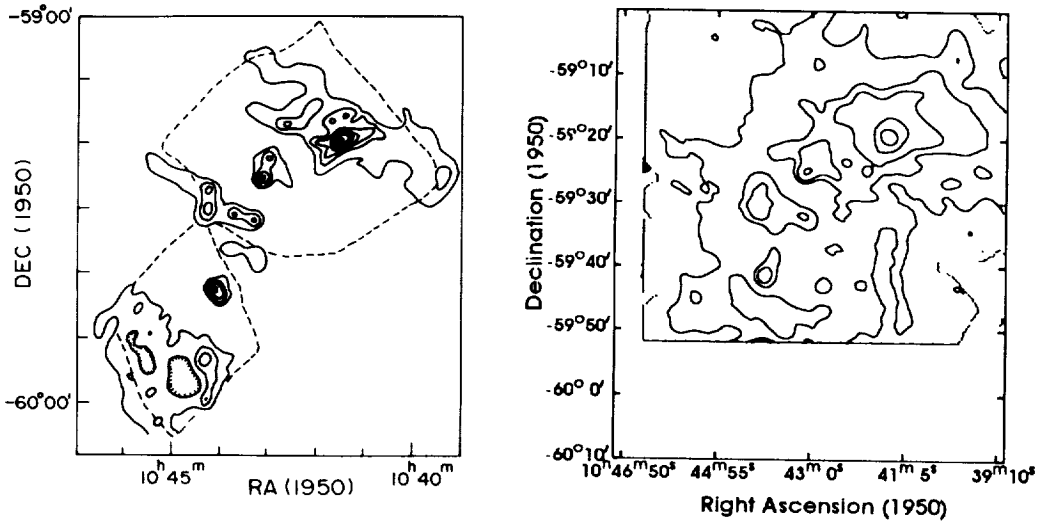

FIGURE 1 Intensity distribution for Carina nebula **a)** at 150 μm from balloon-borne observations deconvolved with MEM(a) **b)** at 100 μm from IRAS survey data with HiRes processing. The contour levels are 0.95, 0.5, 0.3, 0.1, 0.05 and 0.01 of the peak.

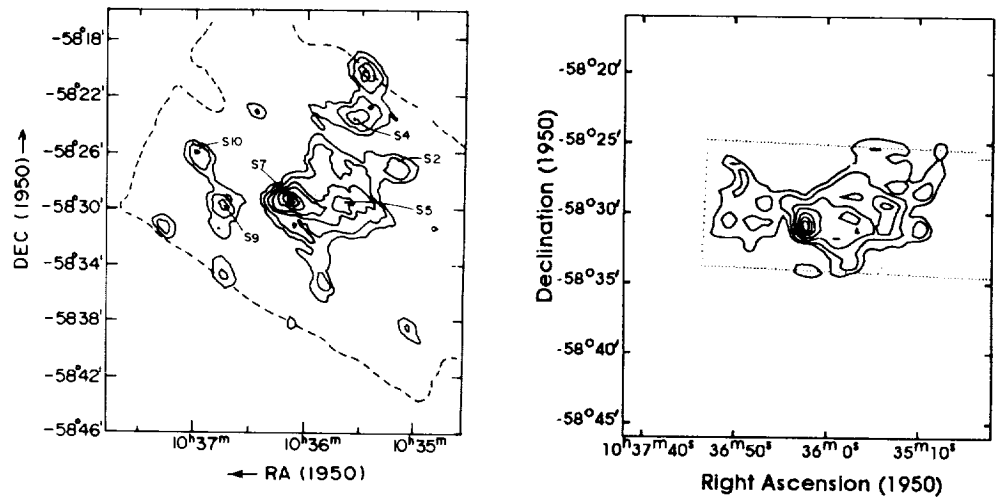

FIGURE 2 Intensity distribution for a region around IRAS 10361–5830 at 60 μm; **a)** from balloon-borne observations; and **b)** from AO data with DSD01A grid processed through MEM(b). The contour levels are 0.9, 0.7, 0.5, 0.3, 0.2, 0.1, and 0.05 of the peak.

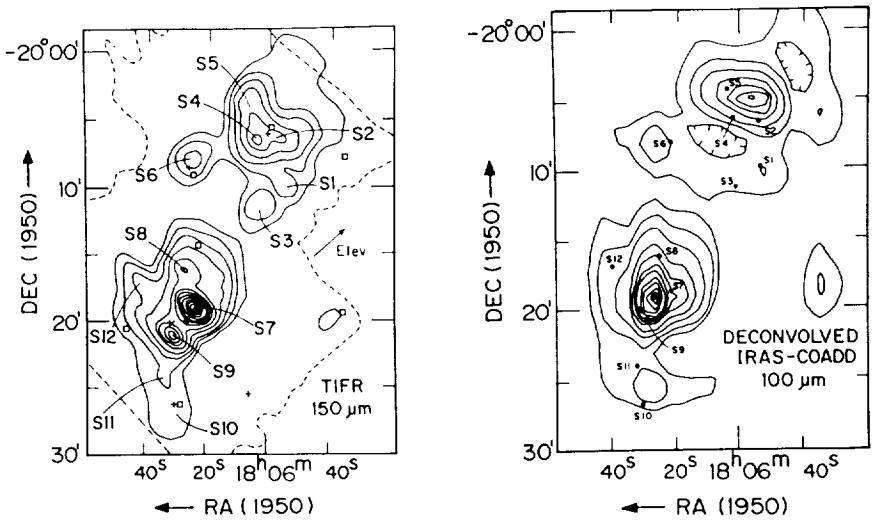

FIGURE 3 Intensity distribution of W31 region **a)** at 150 μm from balloon-borne observations with MEM(a); and **b)** at 100 μm from COADD data deconvolved with MEM(b). The contour levels are 0.95, 0.9, 0.8, 0.7, 0.6, 0.5, 0.4, 0.3, 0.2, 0.1, 0.05, 0.025 and 0.01 of the peak.

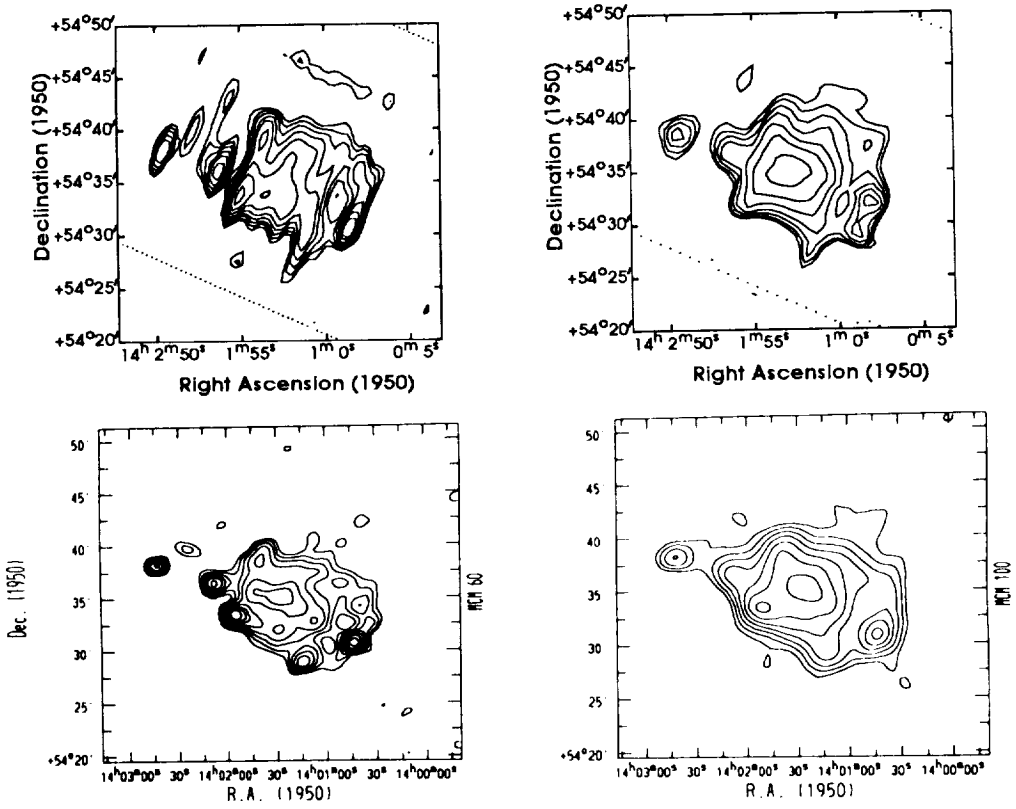

FIGURE 4 Intensity distribution for M101; **a)**, **b)** at 60 μm and 100 μm from AO MEM(b); **c)**, **d)** at 60 μm and 100 μm from HiRes. The contour levels are scaled by a factor of $\sqrt{3}$.

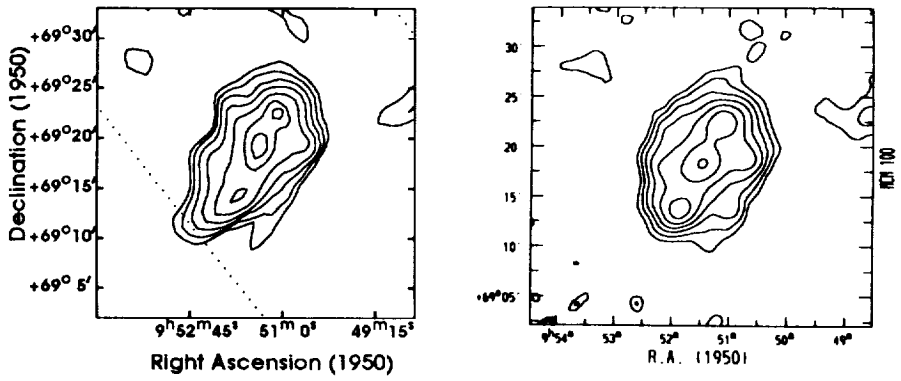

FIGURE 5 Intensity distribution at 100 μm for M81; **a)** from AO MEM; and **b)** from HiRes. The contour levels are scaled by a factor of $\sqrt{3}$.

2. MEM deconvolution of averaged IRAS data from AOs, MEM(b), gives a resolution comparable to that obtained from HiRes processing. However, the dynamic range in the HiRes processing is superior to that of the MEM maps. MEM processing is computationally inexpensive as compared to HiRes processing.

ACKNOWLEDGMENTS

We thank the Infrared Processing and Analysis Center (IPAC) for providing IRAS data and HiRes data processing.

REFERENCES

Aumann, H. H., Fowler, J. W. and Melnyk, M. 1990, *AJ*, **99**, 1674

Ghosh, S. K., Iyengar, K. V. K., Rengarajan, T. N., Tandon, S. N., Verma, R. P. and Daniel, R. R. 1988, *ApJ*, **330**, 928

Ghosh, S. K., Verma, R. P., Rengarajan, T. N., Das, B. and Saraiya, H.T. 1993, *ApJS*, **86**, 401

Gull, S. F. and Daniell, G. J. 1978, Nature, **272**, 686

IRAS Catalogs and Atlases: Explanatory Supplement 1988, ed. C.A. Beichman, G. Neugebauer, H.J. Habing, P.E. Clegg, and T.J. Chester (Washington, DC: GPO)

Rice, W. 1993, *AJ*, **105**, 67

Skilling, J. and Bryan, R. K. 1984, *MNRAS*, **211**, 111